International Journal of Scientific Research in Science and Technology
Print ISSN: 2395-6011 | Online ISSN: 2395-602X (www.ijsrst.com)
© 2021 | IJSRST | Volume 8 - Issue 1

High Gas Sensor Performance of Spinel-Type $Zn_{0.7}Mg_{0.3}Co_2O_4$ Nanoparticles Prepared by sol-gel method

T. R. Tatte[a], V.D. Kapse[b]

[a]Department of Physics, Shri. Dr. R. G. Rathod Arts and Science College, Murtizapur, Maharashtra, India

[b]Department of Physics, Arts, Science and Commerce College, Chikhaldara, Maharashtra, India

ABSTRACT

This work devotes to investigate synthesis of spinel $Zn_{0.7}Mg_{0.3}Co_2O_4$ structure was successfully synthesized by sol–gel method. Surface morphology was examined by means of Scanning electron microscopy (SEM). The gas sensing investigations revealed that $Zn_{0.7}Mg_{0.3}Co_2O_4$ nanostructures based gas sensor exhibited high response (50 ppm) and selectivity towards hydrogen sulfide. Besides, enhanced gas sensing properties of $Zn_{0.7}Mg_{0.3}Co_2O_4$ nanostructures are observed. The excellent gas sensing characteristics of $Zn_{0.7}Mg_{0.3}Co_2O_4$ nanostructures might be attributed to their high porosity and large specific surface area. Moreover, hydrogen sulfide gas sensing mechanism was proposed to explain the high sensor response.

Keywords : Sol–gel; Oxalic acid; Spinel; $Zn_{0.7}Mg_{0.3}Co_2O_4$; XRD.

I. INTRODUCTION

Rapid technological and industrial developments continuously result in the emission of hazardous gases, toxins, harmful, flammable and explosive gases and biomolecules. Therefore, sensing of such undesirable chemical or biochemical forms has become a significant research endeavor in recent years [1–3]. The effective detection and removal of toxic gases in the atmosphere is important for human as well as any living organisms. The uncontrolled release of toxic gases such as CO, H_2S, NH_3, CH_3CH_2OH, etc. from automobiles, industries, laboratories, etc. cause severe health problems and they may even cause death [4-6]. Advanced sensing materials have been adopted in this context to achieve high responsivity combined with less response/recovery time and continuous detection of gas molecules for gas sensors, which are key quality factors that define the sensor performance. In particular, oxides are extensively researched for gas sensing, in view of their robust material properties and their ability to change valence through charge transfer [7-9].

Nanocrystalline $ZnCo_2O_4$ has also been applied as electro catalyst for many anodic processes such as oxygen evolution [10], photocatalyst [11] and semiconductor gas sensor [12]. In cobalt based $ZnCo_2O_4$ cubic spinel structure, where Zn divalent ions occupy the tetrahedral and Co trivalent ions occupy octahedral site [13]. Nanostructured $ZnCo_2O_4$ is stable and cheaper than nobel metals [14]. Moreover, it is also active in alkaline solutions.

In this work, we present the synthesis and study of the gas sensing properties of $Zn_{0.7}Mg_{0.3}Co_2O_4$ nanomaterial for the detection of H_2S. The operating temperature of the material and its interaction mechanism with the H_2S has a crucial effect on the response and selectivity of the sensing device. The results obtained show that the $Zn_{0.7}Mg_{0.3}Co_2O_4$ nanostructure exhibits an excellent sensing performance for potential applications in H_2S gas sensors.

II. EXPERIMENTAL

2.1 Preparation of $Zn_{0.7}Mg_{0.3}Co_2O_4$ powder

The appropriate amounts of start materials $Co(NO_3)_2{\cdot}6H_2O$ (99.0%) and $Zn(NO_3)_2{\cdot}6H_2O$ (99.0%) were dissolved in ethanol (95.0%), mixed well with each other, and then slowly adding ethanol solution of oxalic acid (99.8%) at room temperature under constant magnetic stirring. The mixture was then stirred for 3 h and then evaporated at 80 ^{0}C for 1 h under constant stirring, which led to the formation of a sol. The sol was heated at 100^{0}C for 1 h until a gel was formed. Subsequently dried for 1 h in an electric oven and ground the gel, thus the oxalate precursor powder was attained. The resulting material was calcined at 500^{0}C for 2 h and well-crystallized spinel $Zn_{0.7}Mg_{0.3}Co_2O_4$ powder was obtained.

2.2. Fabrication of sensor

Appropriate quantity of mixture of organic solvents such as butyl cellulose, butyl carbitol acetate and turpineol was added to the mixture of $Zn_{0.7}Mg_{0.3}Co_2O_4$ and a solution of ethyl cellulose (a temporary binder). The mixture was then ground to form paste. The paste obtained was screen printed onto a glass substrate in desired patterns. The thick films so prepared were fired at 500°C for 1h.

III. RESULT AND DISCUSSION

3.1. X-ray powder diffraction (XRD) analysis

Fig. 1 shows the XRD pattern of the synthesized $Zn_{0.7}Mg_{0.3}Co_2O_4$ nanomaterial at 500^{0}C for 2 h. It exhibits the diffraction peaks appeared at 2θ values 19.6^0, 31.15^0, 36.711^0, 63.06^0, 65.047^0 and 68.0^0 correspond to the crystal planes of (111), (220), (311), (222), (422), (511), (440), (620), (533) and (622) respectively which confirms the formation of pure $Zn_{0.7}Mg_{0.3}Co_2O_4$ spinel structure. The crystallite size was calculated by using the Debye–Scherrer equation.

$$D = \frac{k\lambda}{B\cos\theta} \quad (1)$$

Where, D is the average size of the crystallite, assuming that the grains are spherical, k is 0.9, λ is the wavelength of X-ray radiation, B is the peak full width at half maximum (FWHM) and θ is the angle of diffraction. The crystalline size of the calcined mixed precursor is found to be 18 nm.

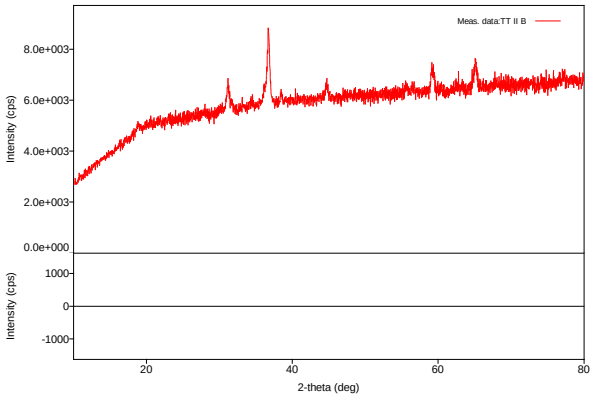

Fig. 1. XRD patterns of $Zn_{0.7}Mg_{0.3}Co_2O_4$ annealed at 500^{0}C.

3.2. Fourier transform-Infrared spectra (FT-IR) analysis

$Zn_{0.7}Mg_{0.3}Co_2O_4$ powder spectrum presented in Fig. 2. From Fig. 2, it can be obtained that the peak at 667 cm–1 is attributed to the stretching vibration mode of M–O for the tetrahedrally coordinated metal ions. The

band at 573 cm–1 can be assigned to the octahedrally coordinated metal ions.

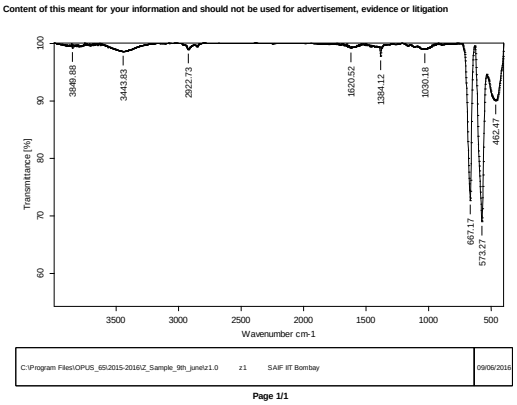

Fig. 2. FTIR spectrum of $Zn_{0.7}Mg_{0.3}Co_2O_4$ powder.

3.3. Scanning electron microscopy (SEM) analysis

Fig. 3 depicts SEM image of $Zn_{0.7}Mg_{0.3}Co_2O_4$ thick film. It can be observed that $Zn_{0.7}Mg_{0.3}Co_2O_4$ thick film show structure having large grains size with soft agglomerations has a regular morphology (polygons).

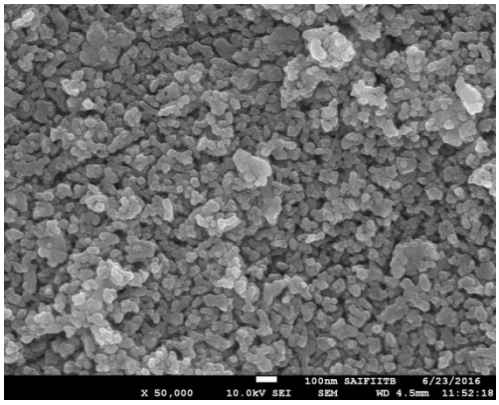

Fig. 3. SEM image of nanosized $Zn_{0.7}Mg_{0.3}Co_2O_4$.

3.4. Energy dispersion X-ray (EDX) analysis

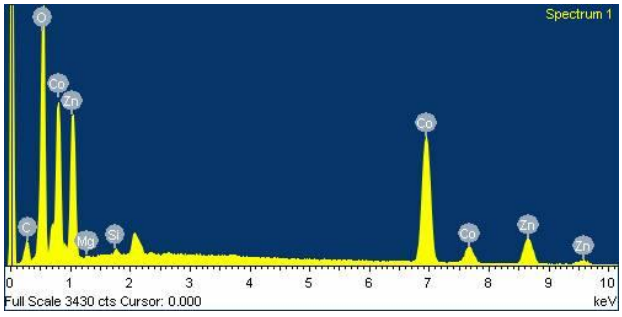

Fig. 4. EDX spectrum for nanosized $Zn_{0.7}Mg_{0.3}Co_2O_4$.

Fig. 4 shows EDX patterns of the nanosized spinel $Zn_{0.7}Mg_{0.3}Co_2O_4$. From the EDX spectrum, the presence of Zn, Co and O elements alone in the sample, has been confirmed the absence of any other impurities.

3.5 Transmission electron microscopy (TEM) analysis

The TEM image of the $Zn_{0.7}Mg_{0.3}Co_2O_4$ calcined at 500 ^{0}C for 2 h are shown in Fig. 5(a). It indicates the presence of $Zn_{0.7}Mg_{0.3}Co_2O_4$ nanoparticles with size 30–40 nm which form beed type of oriental aggregation throughout the region.

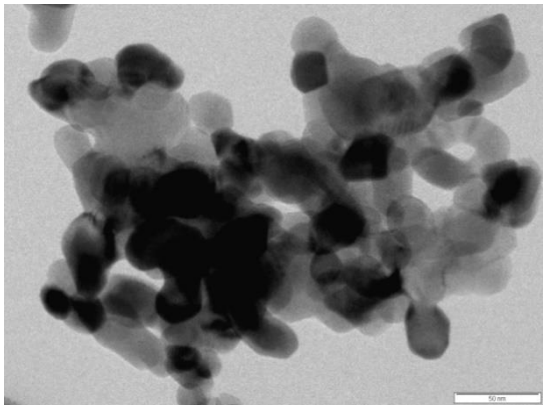

Fig. 5(a). TEM image of nanosized $Zn_{0.7}Mg_{0.3}Co_2O_4$.

Fig. 5(b) shows the selected area electron diffraction (SAED) pattern the spot type pattern which is indicative of the presence of single crystallite particles.

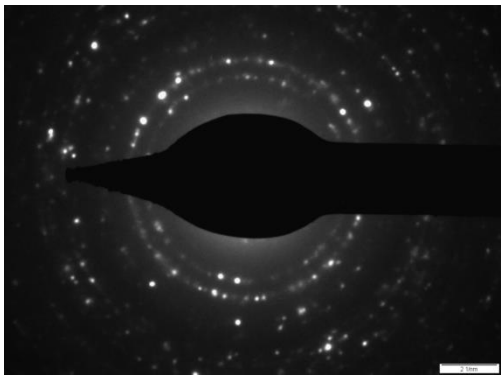

Fig. 5(b). Image of $Zn_{0.7}Mg_{0.3}Co_2O_4$ nanoparticles with SAED pattern.

4. Gas sensing properties

To study the selective behavior of nanocrystalline $Zn_{0.7}Mg_{0.3}Co_2O_4$ gas response (S) towards 50 ppm for

various test gases such as LPG, NH_3, CO_2, H_2S, Cl_2, H_2 and C_2H_5OH at optimal operating temperature 100°C and is depicted in Fig. 6.

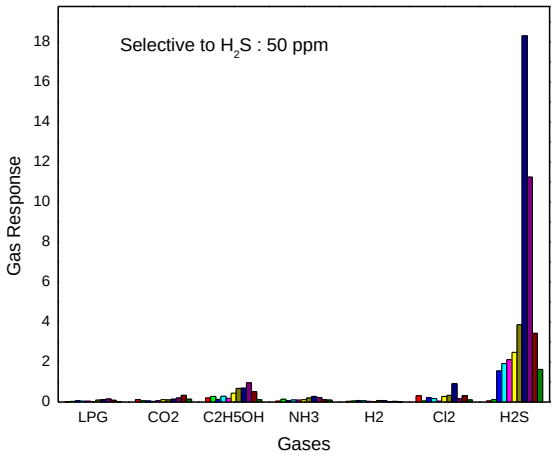

Fig. 6. Selectivity of nanocrystalline $Zn_{0.7}Mg_{0.3}Co_2O_4$ thick films.

The $Zn_{0.7}Mg_{0.3}Co_2O_4$ sample exhibited the higher gas response 18.31 towards H_2S. Hence, the $Zn_{0.7}Mg_{0.3}Co_2O_4$ sensors show maximum selectivity for H_2S gas towards 50 ppm among all the tested gases.

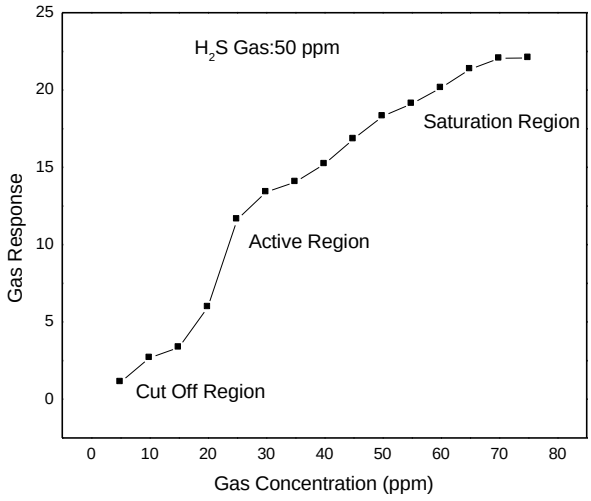

Fig. 7. Gas response of $Zn_{0.7}Mg_{0.3}Co_2O_4$ as a function H_2S concentration.

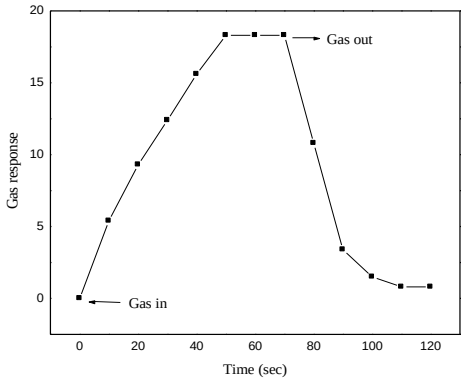

Fig. 8. Response characteristics of $Zn_{0.7}Mg_{0.3}Co_2O_4$ thick film to 50 ppm H_2S

The response of $Zn_{0.7}Mg_{0.3}Co_2O_4$ as a function of H_2S gas concentration at 100°C is shown in Fig. 7. The gas response was observed to increase with increase in the gas concentration and thereafter it remains almost constant. The response and recovery time characteristics of nanocrystalline $Zn_{0.7}Mg_{0.3}Co_2O_4$ based sensor to 50 ppm H_2S at 100°C are depicted in Fig. 8. The nanocrystalline $Zn_{0.7}Mg_{0.3}Co_2O_4$ have quick response time 16 s and fast recovery time 52 s. Therefore, nanocrystalline $Zn_{0.7}Mg_{0.3}Co_2O_4$ based sensor exhibits the good response and recovery time to H_2S.

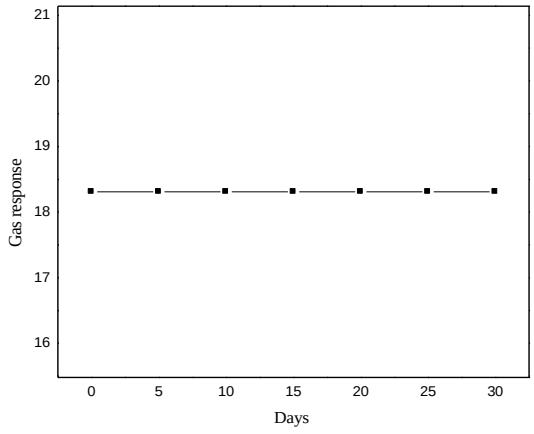

Fig. 9. Stability nanocrystalline $Zn_{0.7}Mg_{0.3}Co_2O_4$ thick film.

The reproducible nature of nanocrystalline $Zn_{0.7}Mg_{0.3}Co_2O_4$ based thick film sensor to 50 ppm H_2S

was measured for a month in the interval of 10 days and result are shown in Fig. 9. From figure, it was found that nanocrystalline $Zn_{0.7}Mg_{0.3}Co_2O_4$ based sensor possesses a very good stability and durability.

IV. CONCLUSION

In summary, we have reported the synthesis and investigations of gas sensing properties of $Zn_{0.7}Mg_{0.3}Co_2O_4$ nanomaterial for the detection of H_2S. The material was fabricated by the sol-gel method. TEM investigation reveals the average crystallite size is in accordance with XRD results. The excellent gas sensing performance of the prepared $Zn_{0.7}Mg_{0.3}Co_2O_4$ nanomaterial was attributed to its morphology, the operating temperature and the disparity in the sensing mechanism between H_2S and other reducing gases. The obtained results demonstrate the potential suitability of the application of $Zn_{0.7}Mg_{0.3}Co_2O_4$ in gas sensing devices for the detection of H_2S.

V. REFERENCES

[1]. K. Wetchakun, T. Samerjai, N. Tamaekong, C. Liewhiran, C. Siriwong, V. Kruefu, A. Wisitsoraat, A. Tuantranont, S. Phanichphant, Sens. Actuators, B, 160 (2011) 580.

[2]. J. Zhang, Z. Qin, D. Zeng, C. Xie, Phys. Chem. Chem. Phys., 19 (2017) 6313.

[3]. G. Korotcenkov, Mater. Sci. Eng., B, 139 (2007) 1.

[4]. A. M. Azad, S. A. Akbar, S. G. Mhaisalkar, et al., J Electrochem Soc., 139 (1992) 3690.

[5]. R. W. Bogue, Meas Sci Technol., 1(1996) 1.

[6]. Y. R. Wu, J. Singh, Appl. Phys. Lett., 85 (2004) 1223.

[7]. N. Barsan, D. Koziej, U. Weimar, Sens. Actuators, B, 121 (2007) 18.

[8]. Q. Wang, X. Li, F. Liu, C. Liu, T. Su, J. Lin, P. Sun, Y. Sun, F. Liu, G. Lu, RSC Adv., 6 (2016) 80455.

[9]. C. Wang, L. Yin, L. Zhang, D. Xiang, R. Gao, Sensors, 10 (2010) 2088.

[10]. B. Chi, J. Li, X. Yang, H. Lin, N. Wang, Electrochim. Acta, 50 (2005) 2059.

[11]. S. V. Bangale, R. D. Prashale, S. R. Bamane, J. Chem. Pharm. Res., 3 (2011) 527.

[12]. X. Niu, W. Du, W. Du, Sens. Actuators, B, 99 (2004) 405.

[13]. K. Karthikeyan, D. Kalpana, N. G. Renganathan, Ionics, 15 (2009) 107.

[14]. S. Trasatti, J. Lipkowski, P. N. Ross, The Electrochemistry of Novel Materials, VCH Publishers, Weinheim, (1994) 207.